Responses to RC1

Dear reviewer,

We sincerely appreciate your constructive comments, which have significantly contributed to the improvement of our manuscript. We have made thorough and detailed revisions according to your suggestions. Please refer to the attached document for a detailed review.

Best regards,
Yi Zhou and other co-authors.

This manuscript, titled "Seasonal evolution and parameterization of Arctic sea ice bulk density: results from the MOSAiC expedition and ICESat-2/ATLAS", deals with the sea ice density, which is a key issue in estimating the sea ice thickness in satellite altimetry. I consider it novel to use MOSAiC data for informing us of the seasonal evolution of sea ice density. And the majority of the analysis and result is sound. However, several major issues have to be made, which are listed below.

Authors' response: Thank you for your thorough analysis and insightful feedback on our manuscript. We have carefully considered and addressed each of the major issues you highlighted. Additionally, we have integrated suggestions from other members of the *EGU Community* to further enhance the quality and accuracy of our work. Overall, we have reassessed all the results and a brief list of refinements can be found in ***Supplementary A1*** (at the end).

First, the spatial representation issue is central to the analysis, and has to be dealt with in a more systematic way. The two particular sources of uncertainty in Eqs. 5 are that of hf (total freeboard) and rho_s (snow density). For example, for hf and the analysis with buoy-measured hi and hs in Fig. 3, the uncertainty is actually two fold, under formal definitions. First, the uncertainty between the mode of the log-normal fitted IS2 hf and the areal mean level-ice hf, and second, that between the areal mean level-ice hf and that measured at the buoy (in order to compare with buoy hi & hs). The total uncertainty addressed here is only the difference between fitted mode and the maximum probability bin of hf. This uncertainty falls into part of the first uncertainty I mentioned, and hence the second uncertainty is not accounted for. The representation error in snow depth is potentially large as well, but could diminish more quickly at larger scales. The representation issue is also raised by two community comments.

Authors' response: We agree with the reviewer's suggestion that the spatial representation of buoy arrays and satellite measurements needs to be better coordinated. In addition, we recognize that the uncertainties in the hf (total freeboard) used as an input to the hydrostatic equilibrium equation need further investigation. In the revised manuscript, we have made significant revisions in this regard, which can be summarized as follows:

a) We evaluated the feasibility of using the modal value of the total freeboard distribution (including all ice types) as a proxy for the mean total freeboard of the level ice. Specifically, we used the latest AWI Icebrid total freeboard data provided by Jutila et al. (2024a) and Jutila et al. (2024b) for detailed analysis and found that the modal freeboard and the mean freeboard for level ice were in very good agreement, demonstrating the robustness of our methodology **(Fig. A1, more details in our responces to CC2)**. This is the first step of our IBD retrieval, where we extract the level ice fraction from the IS2 measurements (i.e., IS2 modal freeboard) to ensure that the measured

sea ice type is consistent with the observations from the IMB array, as all selected IMBs are deployed on the level ice.

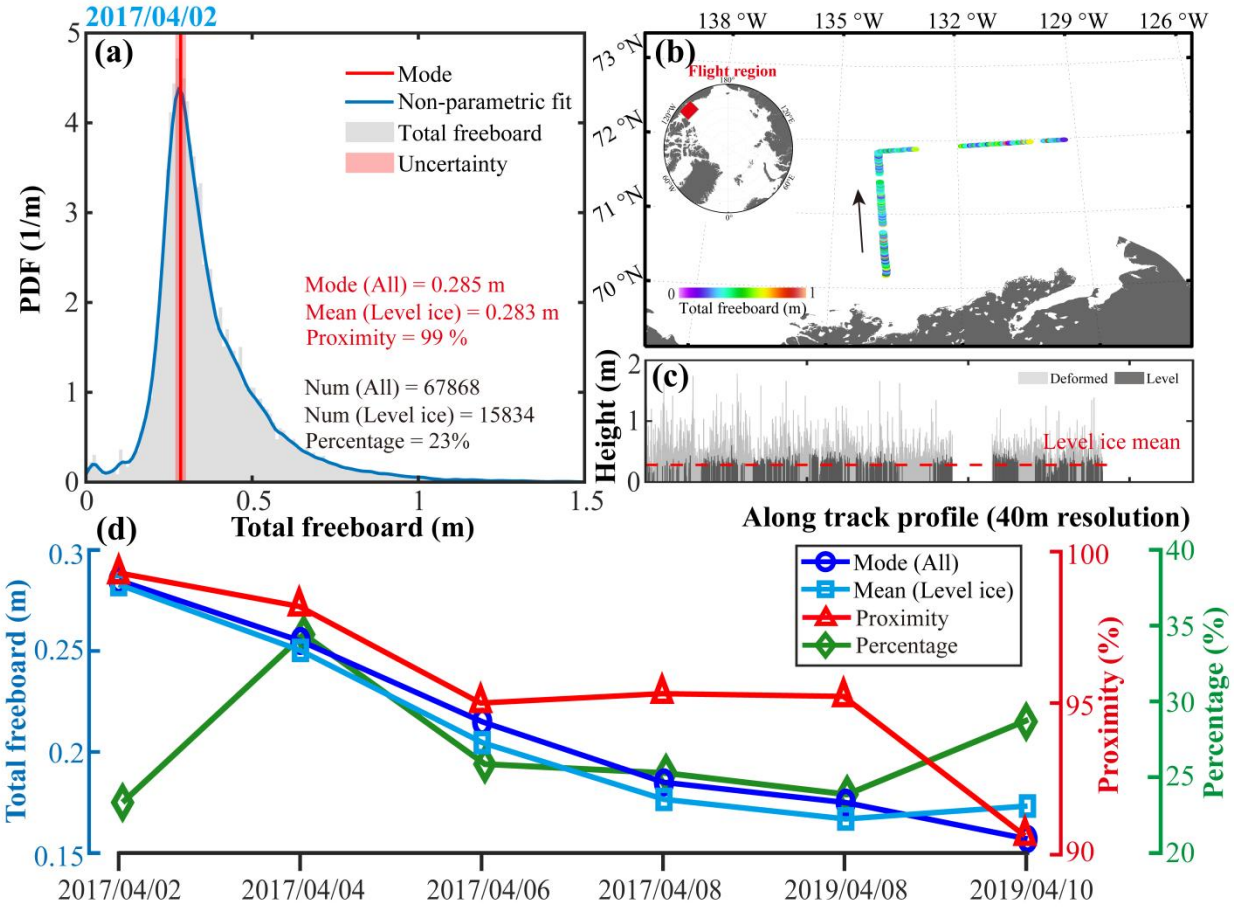

Figure A1. Comparison of the modal value of the total freeboard distribution (all ice types) with the mean total freeboard of level ice from AWI Icebird measurements in 2017 and 2019. The example for 2 April 2017 shows (a) the total freeboard distribution, (b) the measurement area, and (c) the total freeboard profile. (d) Results for each measurement date, including modal freeboard, mean level ice, absolute relative percentage difference between the two (proximity), and proportion of level ice (percentage).

b) We updated the calculation method for the modal freeboard, thereby incorporating a portion of the Type I uncertainty of hf due to the quasi-peak frequency region. In the revised manuscript, we have updated the IS2 data to version 6 and have discontinued the use of 150-segment averaging and log-normal fitting to determine IS2 modal values. Instead, we have maintained the original resolution of the IS2 data and determined the final IS2 modal freeboard by averaging the top five frequency peaks, with the standard deviation representing the Type I uncertainty. This modification aims to avoid introducing additional fitting and averaging constraints that could impact the original distribution characteristics of the IS2 data. Figure A2 presents several examples of the IS2 freeboard distribution, illustrating the modal freeboard (red line) and its associated uncertainty(red shaded band). In addition, we also introduced airborne laser scanning (ALS) data during MOSAiC to complement the L-site scale (25km radius from CO) analysis (see also Fig. A2).

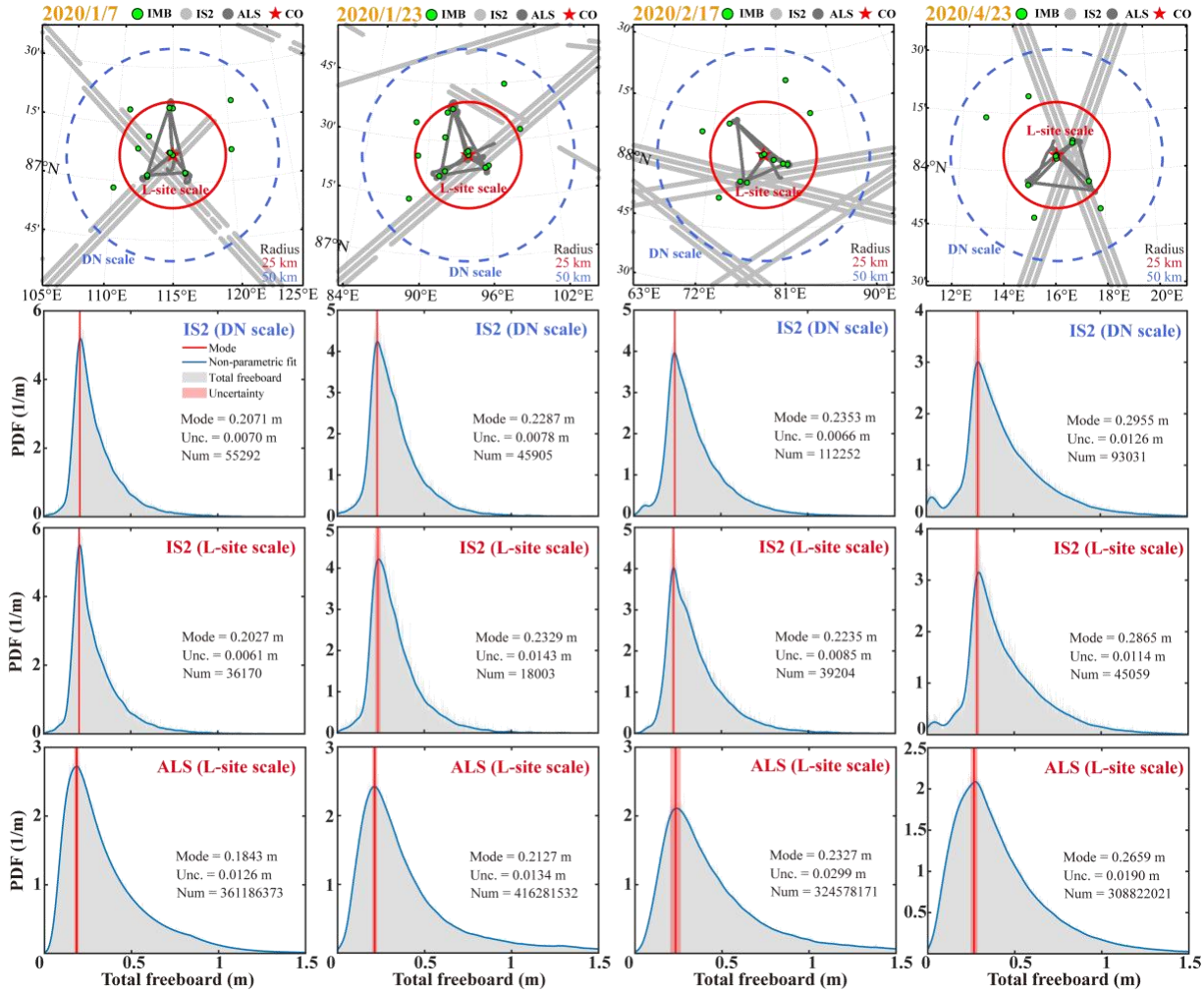

Figure A2. Distribution of IS2, ALS, and IMB array measurements, showing the cases on January 7, 2020, January 23, 2020, February 17, 2020, and April 23, 2020.

c) The difference between the IS2 modal freeboard and the reference modal freeboard was used as a supplement to the Type I uncertainty. With the introduction of ALS data, which offered in-situ measurements with higher resolution and accuracy compared to IS2, we used the ALS modal freeboard as a reference to evaluate the IS2 modal freeboard. However, it must be acknowledged that airborne data also have inherent biases, but using airborne data to evaluate satellite data is a common practice. Considering that the ALS data only cover the L-site scale, we screened all IS2 data for dates with sufficient data points (more than 15,000 segments) for comparison. Ultimately, four effective date records were identified, as shown in Figure A2. We calculated the average deviation of the modal freeboard between ALS and IS2 for these dates, estimated to be ~0.0125 m, and incorporated this into the Type I uncertainty for IS2 modal freeboard.

d) Coordination of spatial scales between the buoy array and IS2 measurements (Type II uncertainty). To retrieve IBD based on the hydrostatic equilibrium equation, the satellite (or airborne) modal freeboard and the mean ice thickness and snow depth from the buoys need to achieve spatial coordination. However, to directly examine the spatial scale differences between the buoy array and satellite measurements, it is necessary to ensure that both scales have the same type of sea ice parameters (and at least some records), but this condition is currently not met. Therefore, we adopted an indirect method by introducing a spatial scale correction term to harmonize the

measurements from the two scales, and thus the type II uncertainty was considered as a correction term. The details are as follows:

(1) We compared the buoy array data with transects covering a larger measurement area and found that the trends in mean snow depth (surface ice only) were very close at both scales (Fig. A2(c)). Furthermore, according to Koo et al. (2021), the trend in the IS2-derived mode thickness was also found to be very close to that of the average thickness measured by the buoy array. Therefore, we expect that the buoy array will be able to capture variations in sea ice and snow over a spatial area larger than the buoy deployment sites, which serves as a fundamental basis for our subsequent spatial correction.

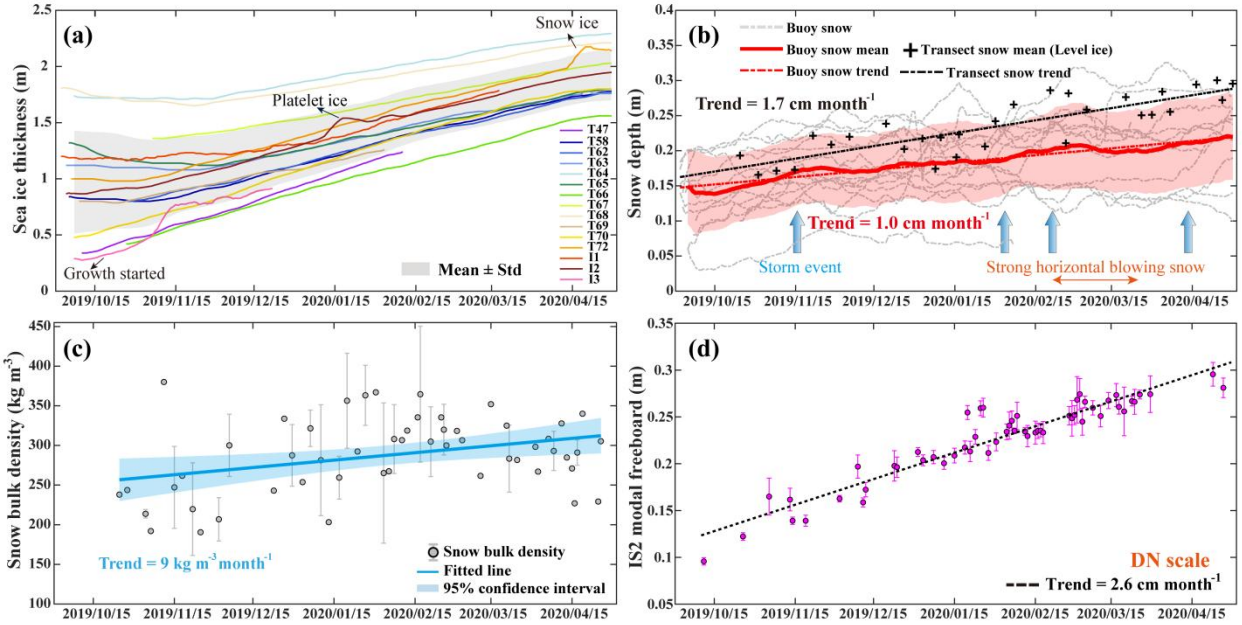

Figure A3. Variations of sea ice and snow during the MOSAiC freezing season (DN scale). (a) Sea ice thickness measurements from the IMBs. The peculiarities of T72, I2, and I3 sites (as described in the text) are indicated by black arrows. The gray shaded band indicates the mean ± standard deviation (at least 10 buoys). (b) Snow depth measurements obtained from buoys and transects. The blue arrows mark four storm events, and the yellow arrow indicates a period characterized by a strong snow drifting event, according to Wagner et al. (2022). (c) Snow bulk density derived from snow pit measurements. (d) Seasonal evolution of the IS2 modal freeboard, with uncertainties indicated by error bands.

(2) We subtracted the mean snow depth of the buoy array from the IS2 mode freeboard to evaluate the resulting sea ice freeboard. Subsequently, we observed a significant negative sea ice freeboard in early autumn, with a trend towards decreasing to zero before gradually increasing again. Based on the ice core data obtained from Oggier et al. (2023a) and Oggier et al. (2023b) (including SYI and FYI), we found that the mean sea ice freeboard was approximately 0.031 m in autumn. Therefore, this indicates that there are indeed systematic differences between the measurements of the buoy array and IS2. Considering their ability to capture similar trends in sea ice variations, we propose using the maximum negative sea ice freeboard and the baseline freeboard (derived from ice core averages) as an empirical correction term to account for the scale differences between the IS2 mode freeboard and the buoy array measurements (simply understood as a systematic uplift of the derived sea ice freeboard). Ultimately, when used for IBD retrieval, the IS2 modal freebord added an additional 0.045 m + 0.031 m to mitigate the issue of scale differences. For the ALS, there is a slight difference, represented as 0.046 m + 0.031 m. The recalculated DN scale IBD variations are shown in Fig. A4.

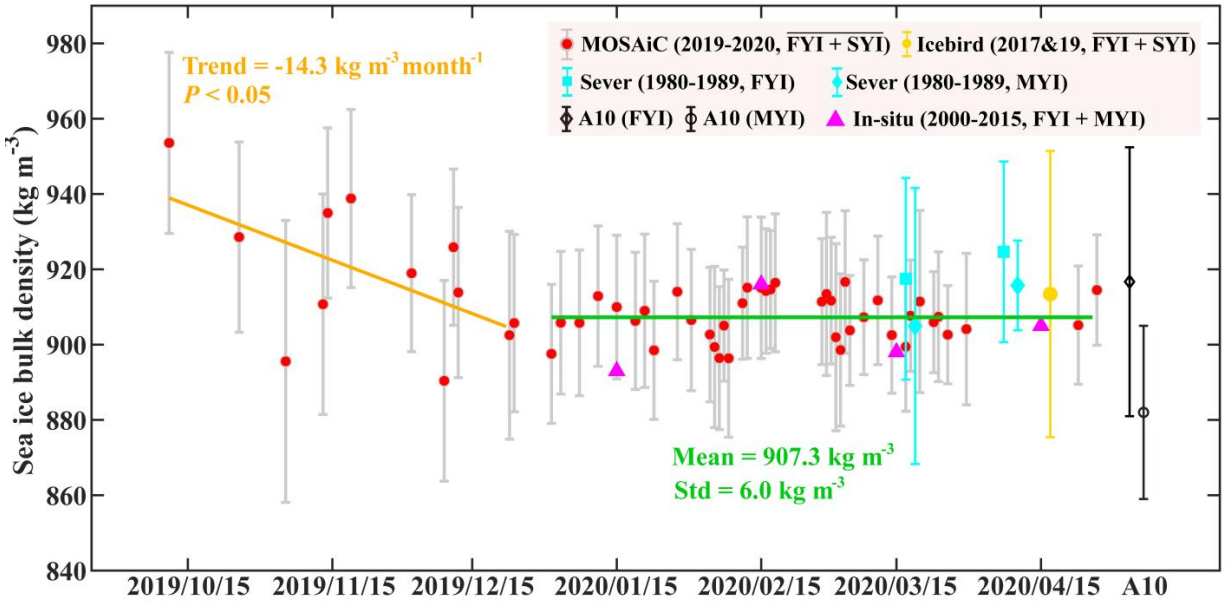

Figure A4. Seasonal evolution of IBD during the MOSAiC freezing season. The orange line indicates a significant decreasing trend in the MOSAiC IBD, while the green line indicates the mean value during a relatively stable phase. Also shown are the mean IBDs of FYI (black diamond) and MYI (black circle) from the A10 climatology (Alexandrov et al., 2010), the mean IBDs of FYI (cyan square) and MYI (diamond) estimated during the Arctic Sever expedition from 1980 to 1989 (Shi et al., 2023), the mean ice densities (FYI and MYI, purple triangle) from 2000 to 2015 based on in situ observations (Ji et al., 2021), and the mean IBD (FYI and SYI, yellow circle) based on AWI Icebird multi-sensor measurements in April 2017 and 2019 (Jutila et al., 2022). The underline indicates IBD results for level ice only. The gray error bars indicate the uncertainty of the MOSAiC IBD, and the other error bars indicate one standard deviation. Note that the density data from the historical measurements correspond to the month, regardless of the year.

Second, and consequently from the first point I raised, the apparent better fitting with the bivariate formulation (Sec. 3.3 and Fig. 7). One should be very careful in claiming that any fitting is better for parameterizing the ice density. Since if one look closely at Eqs. 5 and the first point I raised, it is immediate that the representation uncertainty will be a major source of correlation (R2>0.9 for both cases) with bivariate formulation, since: rho_i = rho_w*(hi+hs-hf)/hi + ⋯, where (hi+hs-hf) is the derived sea ice draft, and contains a large representation error. This error gets carried to rho_i, in proportions, so that the values on both sides correlates really well (R2=0.9). In a sense rho_i and draft/thickness ratio are NOT independent due to the way rho_i is derived. And more importantly, the representation uncertainty dominates over the variability in the snow-related, second term in Eqs. 5. Let me be very clear here: I think there should exist significant correlation between the rho_i and draft/thickness ratio, which could arises from physical reasons (see also IceBird results in Sec. 4.4). I just don't consider the argument here to be strict enough for comparing the parameterization schemes for ice density, and especially, whether the bivariates are better. Better quantification of uncertainty due to limited representation, is potentially needed before such claims.

Authors' response: We agree with your point that the better fit of the bivariate parameters does not necessarily mean that they are the best parameters to determine IBD. We will thoroughly discuss issues related to fit uncertainty, physical dependence and error propagation in the revised manuscript. However, based on the significant revisions in the IS2 modal freeboard and associated uncertainties, we have updated the IBD parameterisation scheme and provided more details. The new IBD parameterisations show a generally reduced correlation compared to the

original results (Fig. A5). This implies that the added uncertainty and scale corrections have reduced the error dependence between the sea ice parameters and the retrieved IBD.

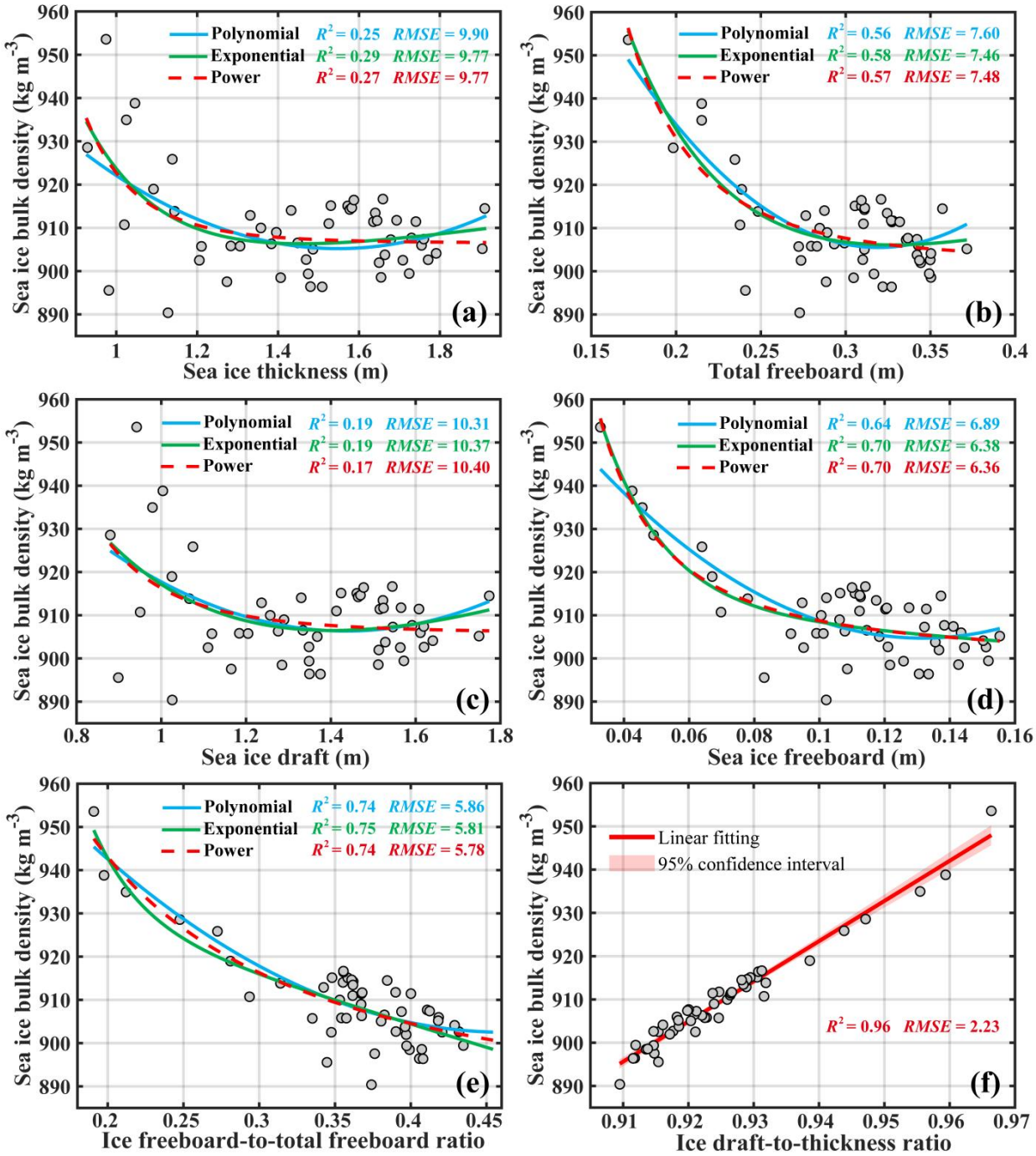

Figure A5. Parameterization of the IBD, including regression models using (a) sea ice thickness, (b) total freeboard, (c) sea ice draft, (d) sea ice freeboard, (e) ice freeboard-to-total freeboard ratio, and (f) ice draft-to-thickness ratio. Each panel shows model fit metrics, including the coefficient of determination (R^2) and the root mean square error (*RMSE*). Note that the statistical *P*-value for all results is less than 0.05 and the unit of *RMSE* is in kg m^{-3}.

Third, I think better sea ice topography data collected during MOSAiC campaign serve as a very good source of information for this study, which is a point already raised by Arttu (in first CC). However, maybe the dataset does not fully support the study of the whole winter, but it is definitely worth to look into and discussed in the paper.

Authors' response: We agree with the reviewer's suggestions. In the revised manuscript, we have included the MOSAiC ALS data and additionally retrieved the IBD results from the L-site scale (Fig. A2). We used all available buoys within the L-site scale as well as the available IS2 and ALS modal freeboards to retrieve IBD. On this basis, we compared the different sea ice parameters from the DN scale and the L-site scale (Fig. A6).

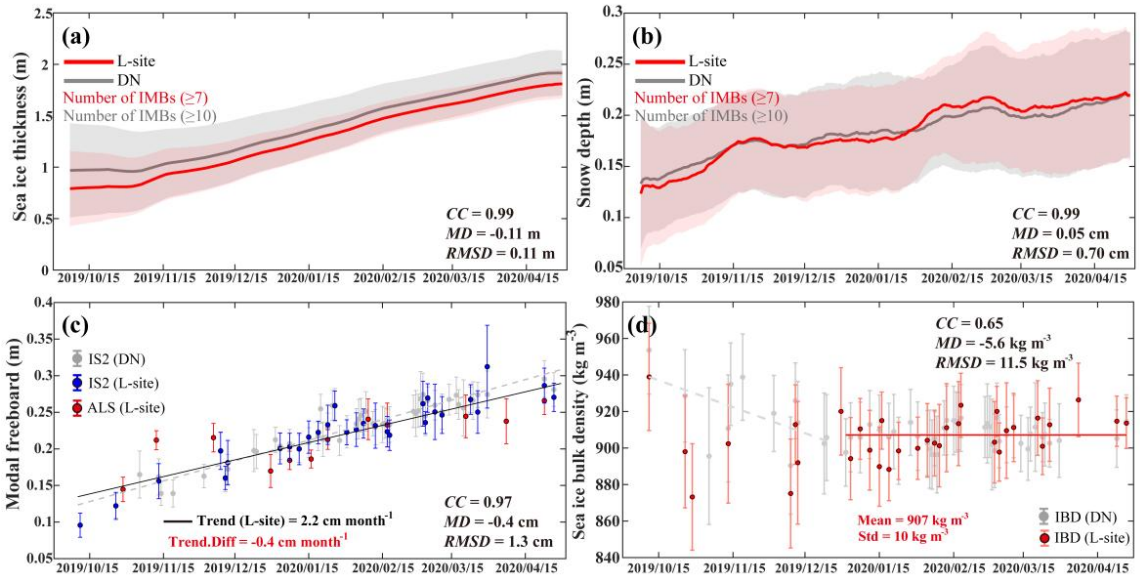

Figure A6. Comparison of L-site and DN sea ice parameters, including (a) sea ice thickness, (b) snow depth, (c) modal freeboard, and (d) sea ice bulk density. Statistical metrics include correlation coefficient (CC), mean difference (MD, L-site minus DN), and root mean square difference (RMSD).

Fourth, I consider the use of IceBird data could be improved. The scale dependency analysis is nice, but one has to be clear of two aspects. First, the uncertainty of SnowRadar (hence hs) and EM (hence hi+hs) over rough ice, which could compromise the analysis for this particularly important ice type. Second, the potential of apparent but superficial statistical correlation since the derived rho_i carries the measurement and representation error of the original measurements. Therefore, I suggest to change the analysis to level ice only with IceBird data, since such type info is available.

Authors' response: Thank you for your comments and suggestions. We have revised our use of the AWI Icebird data accordingly. We have re-calculated the mean IBD of SYI and FYI, including only level ice, from the Icebird data to compare with our results, as shown in Fig. A4. Overall, the IBD from MOSAiC during the relatively stable phase is very close to the IBD from Icebird. Furthermore, in the further analysis of the IBD parameterization using the Icebird sea ice parameters, we have detailed the results for different sea ice types (FYI, SYI and MYI), surface characteristics (rough and level ice), and spatial scales (40 m, 800 m, 12.5 km and 25 km), as shown in Fig. A7 and Fig. A8.

A minor comment: on line 452: the increase of hf may well be due to thermodynamic growth of ice, but purely/largely due to snow accumulation. So be more strict, as follows: These findings indicate that the magnitude of sea ice elevation changes exhibits significant spatial variability, possibly related to initial ice thickness, sea ice growth, and snow accumulation.

Authors' response: Thank you for your clarification and suggestions. We have reorganized this sentence in the revised manuscript.

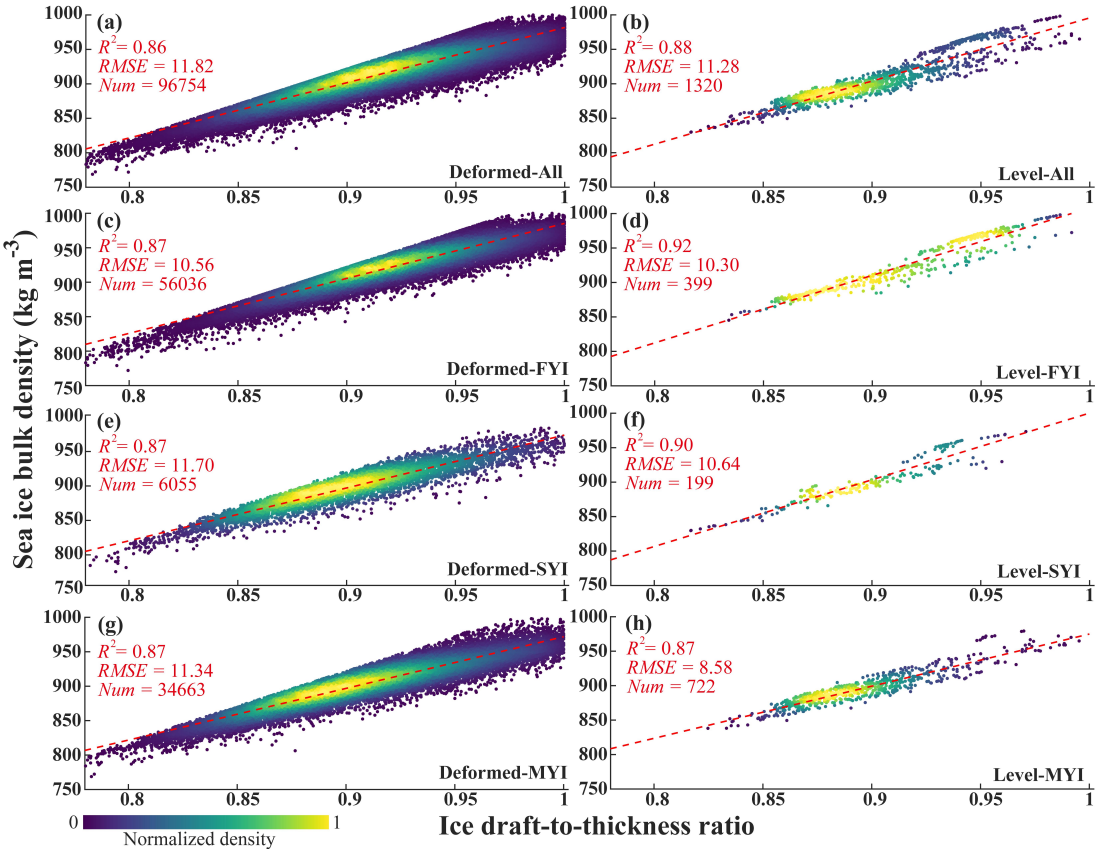

Figure A7. Fitting performance of the ice draft-to-thickness ratio to the IBD at different sea ice types and surface characteristics based on AWI Icebird multi-sensor sea ice data (original resolution), including the results from (a) deformed and all ice types, (b) level and all ice types, (c) deformed and FYI, (d) level and FYI, (e) deformed and SYI, (f) level and SYI, (g) deformed and MYI, and (h) level and MYI.

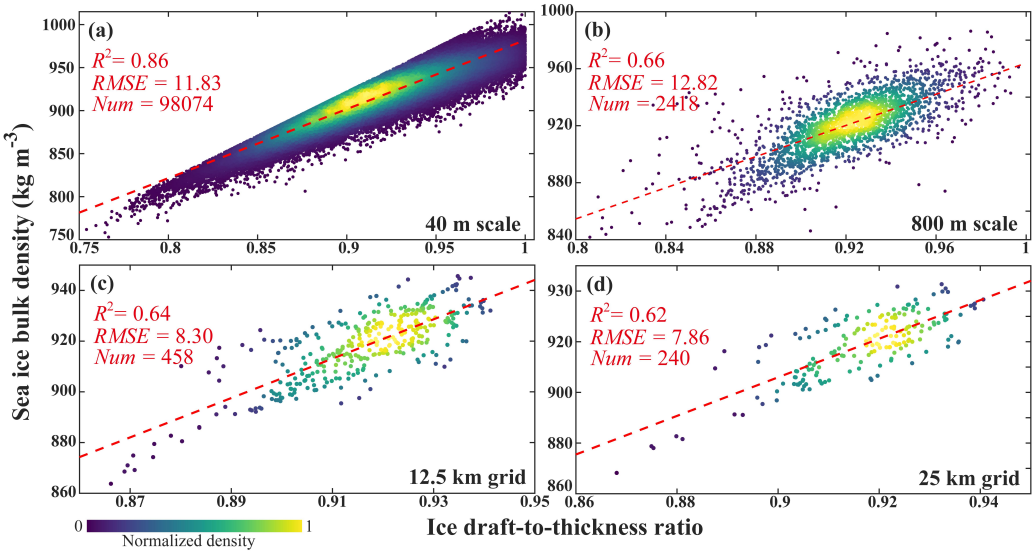

Figure A8. Fitting performance of the ice draft-to-thickness ratio to the IBD at different spatial scales based on AWI Icebird multi-sensor sea ice data, including the results from (a) 40 m, (b) 800 m, (c) 12.5 km, and (d) 25 km.

Supplementary A1

[Data]

a) IS2 Freeboard Data Updated to ATL10 version 6.

Kwok et al. (2023), ATLAS/ICESat-2 L3A Sea Ice Freeboard, Version 6. [Data Set]. NSIDC.(https://doi.org/10.5067/ATLAS/ATL10.006).

b) Airborne Laser Scanning (ALS) Data: Added L-site scale data during the MOSAiC freezing season.

Hutter et al. (2023), Gridded segments from helicopter-borne laser scanner during MOSAiC. [PANGAEA](https://doi.org/10.1594/PANGAEA.950339).

c) AWI IceBird Multi-Sensor Sea Ice Parameters Updated to the Latest Version

- Jutila et al. (2024), Airborne sea ice parameters during the IceBird Winter 2019 campaign in the Arctic Ocean, Version 2. [PANGAEA](https://doi.org/10.1594/PANGAEA.966057).

- Jutila et al. (2024),Airborne sea ice parameters during the PAMARCMIP2017 campaign in the Arctic Ocean, Version 2. [PANGAEA](https://doi.org/10.1594/PANGAEA.966009).

d) Core-Based Ice Density Data: Added data on sea ice density from the *Sea Ice Physics Group* during MOSAiC legs 1 to 4.

- Oggier et al. (2023), First-year sea-ice salinity, temperature, density, oxygen and hydrogen isotope composition from the main coring site (MCS-FYI) during MOSAiC legs 1 to 4 in 2019/2020. [PANGAEA](https://doi.org/10.1594/PANGAEA.956732).

- Oggier et al. (2023), Second-year sea-ice salinity, temperature, density, oxygen and hydrogen isotope composition from the main coring site (MCS-SYI) during MOSAiC legs 1 to 4 in 2019/2020. [PANGAEA](https://doi.org/10.1594/PANGAEA.959830).

[Method]

a) IS2 Modal Freeboard Calculation: In the revised manuscript, we have retained the original resolution of IS2 ATL10 v6 and no longer perform the 150-segment averaging. Additionally, we no longer use log-normal fitting to estimate modal freeboard. Instead, we directly use the average of the freeboard values corresponding to the five highest frequencies in the freeboard distribution to obtain the modal freeboard (standard deviation is used as the uncertainty for the quasi-peak region of the total freeboard distribution). The purpose of this modification is to preserve the original distribution characteristics of the data as much as possible, without imposing fitting constraints or making resolution adjustments. Moreover, we have adopted the same approach to obtain the modal ALS freeboard.

b) Modal Value Feasibility for Level Ice: The AWI Icebird dataset was utilized to assess the feasibility of our approach, which features rigorously defined ice surface classification labels. We obtained the modal freeboard from the total freeboard distribution that includes both level and rough ice, and compared it with the average total freeboard of level ice.

c) Spatial Scale Correction: We introduced a spatial scale correction term to better align buoy array data with IS2/ALS modal freeboards.

d) Added Uncertainty for IS2 Modal Freeboard: We added uncertainty to the IS2 modal freeboard by calculating the mean difference (~0.0125 m) between IS2 and reference ALS modal freeboard.

[Results]

a) Sea Ice Bulk Density (IBD) Recalculation: All IBD results have been recalculated and re-evaluated following substantial revisions.

b) Enhanced IBD Parameterizations: Additional details have been included in the IBD parameterizations to improve clarity and accuracy.

c) IBD Results at Different Scales: Besides the DN scale, IBD results have now been extended to include the L-site scale.

d) High-Precision Ice Core Density: Ice core density that we used were obtained using the high-precision hydrostatic weighing method.

e) Expanded Discussion on IBD Uncertainty: More comprehensive discussions have been added regarding the uncertainty of IBD, its seasonal variations, spatial heterogeneity, limitations, and potential applications.

Reference.

Alexandrov, V., Sandven, S., Wahlin, J., and Johannessen, O.: The relation between sea ice thickness and freeboard in the Arctic, The Cryosphere, 4, 373-380, 2010.

Ji, Q., Li, B., Pang, X., Zhao, X., and Lei, R.: Arctic sea ice density observation and its impact on sea ice thickness retrieval from CryoSat–2, Cold Regions Science and Technology, 181, 103177, 2021.

Jutila, A., Hendricks, S., Ricker, R., von Albedyll, L., and Haas, C.: Airborne sea ice parameters during the IceBird Winter 2019 campaign in the Arctic Ocean, Version 2. PANGAEA, 2024a.

Jutila, A., Hendricks, S., Ricker, R., von Albedyll, L., and Haas, C.: Airborne sea ice parameters during the PAMARCMIP2017 campaign in the Arctic Ocean, Version 2. PANGAEA, 2024b.

Jutila, A., Hendricks, S., Ricker, R., von Albedyll, L., Krumpen, T., and Haas, C.: Retrieval and parameterisation of sea-ice bulk density from airborne multi-sensor measurements, The Cryosphere, 16, 259-275, 2022.

Koo, Y., Lei, R., Cheng, Y., Cheng, B., Xie, H., Hoppmann, M., Kurtz, N. T., Ackley, S. F., and Mestas-Nuñez, A. M.: Estimation of thermodynamic and dynamic contributions to sea ice growth in the Central Arctic using ICESat-2 and MOSAiC SIMBA buoy data, Remote Sensing of Environment, 267, 112730, 2021.

Oggier, M., Salganik, E., Whitmore, L., Fong, A. A., Hoppe, C. J. M., Rember, R., Høyland, K. V., Divine, D. V., Gradinger, R., Fons, S. W., Abrahamsson, K., Aguilar-Islas, A. M., Angelopoulos, M., Arndt, S., Balmonte, J. P., Bozzato, D., Bowman, J. S., Castellani, G., Chamberlain, E., Creamean, J., D'Angelo, A., Damm, E., Dumitrascu, A., Eggers, S. L., Gardner, J., Grosfeld, L., Haapala, J., Immerz, A., Kolabutin, N., Lange, B. A., Lei, R., Marsay, C. M., Maus, S., Müller, O., Olsen, L. M., Nuibom, A., Ren, J., Rinke, A., Sheikin, I., Shimanchuk, E., Snoeijs-Leijonmalm, P., Spahic, S., Stefels, J., Torres-Valdés, S., Torstensson, A., Ulfsbo, A., Verdugo, J., Vortkamp, M., Wang, L., Webster, M., Wischnewski, L., and Granskog, M. A.: First-year sea-ice salinity, temperature, density, oxygen and hydrogen isotope composition from the main coring site (MCS-FYI)

during MOSAiC legs 1 to 4 in 2019/2020. PANGAEA, 2023a.

Oggier, M., Salganik, E., Whitmore, L., Fong, A. A., Hoppe, C. J. M., Rember, R., Høyland, K. V., Gradinger, R., Divine, D. V., Fons, S. W., Abrahamsson, K., Aguilar-Islas, A. M., Angelopoulos, M., Arndt, S., Balmonte, J. P., Bozzato, D., Bowman, J. S., Castellani, G., Chamberlain, E., Creamean, J., D'Angelo, A., Damm, E., Dumitrascu, A., Eggers, L., Gardner, J., Grosfeld, L., Haapala, J., Immerz, A., Kolabutin, N., Lange, B. A., Lei, R., Marsay, C. M., Maus, S., Olsen, L. M., Müller, O., Nuibom, A., Ren, J., Rinke, A., Sheikin, I., Shimanchuk, E., Snoeijs-Leijonmalm, P., Spahic, S., Stefels, J., Torres-Valdés, S., Torstensson, A., Ulfsbo, A., Verdugo, J., Vortkamp, M., Wang, L., Webster, M., Wischnewski, L., and Granskog, M. A.: Second-year sea-ice salinity, temperature, density, oxygen and hydrogen isotope composition from the main coring site (MCS-SYI) during MOSAiC legs 1 to 4 in 2019/2020. PANGAEA, 2023b.

Shi, H., Lee, S.-M., Sohn, B.-J., Gasiewski, A. J., Meier, W. N., Dybkjær, G., and Kim, S.-W.: Estimation of snow depth, sea ice thickness and bulk density, and ice freeboard in the Arctic winter by combining CryoSat-2, AVHRR, and AMSR measurements, IEEE Transactions on Geoscience and Remote Sensing, 2023. 2023.

Wagner, D. N., Shupe, M. D., Cox, C., Persson, O. G., Uttal, T., Frey, M. M., Kirchgaessner, A., Schneebeli, M., Jaggi, M., and Macfarlane, A. R.: Snowfall and snow accumulation during the MOSAiC winter and spring seasons, The Cryosphere, 16, 2022.